# Chromite in the central sector of the Eastern Bushveld Complex, South Africa

EUGENE N. CAMERON

*Department of Geology and Geophysics, University of Wisconsin*
*Madison, Wisconsin 53706*

## Abstract

The compositions of chromites in chromite-poor silicate rocks, in chromitites, and in chromitite–silicate rock series from bottom to top of the Critical Zone have been investigated by electron microprobe analysis. In the chromitites of the Lower Critical Zone there is a fairly regular change in composition upward in the stratigraphic sequence, the higher chromitites being lower in Cr/Fe, $Cr/R^{3+}$, and $Mg/R^{2+}$, and higher in $Fe^{3+}/R^{3+}$ than the lower chromitites. In chromitites of the Upper Critical Zone no systematic upward change in composition is shown. Chromites in chromite-poor silicate rocks are, in general, lower in Cr/Fe, $Mg/R^{2+}$, and $Al/R^{3+}$ than chromites in stratigraphically associated chromitites, and higher in $Fe^{3+}/R^{3+}$ and $Cr/R^{3+}$.

Examined in the light of studies of the crystallization of basalts by Hill and Roeder, the data suggest that increase in oxygen fugacity was not responsible for chromite precipitation and cannot account for covariance of chromite and bronzite or olivine. Tectonically-induced changes in total pressure in the magma chamber are suggested as the prime factor in the formation of the extraordinarily persistent chromitites of the Eastern Bushveld Complex.

## Introduction

Investigations during nearly a hundred years have yielded much information on the size, extent, mode of occurrence, and composition of the unrivalled chromite deposits of the Bushveld Complex. Studies have focussed on chromite in the chromitite "seams," especially the thicker ones; much less attention has been given to chromite in thinner seams and in associated silicate-rich rocks. The studies have shown (1) that from bottom to top of the Critical Zone there are changes in the composition of chromite in chromitites, and (2) that in sequences involving both chromite-poor and chromite-rich rocks, the compositions of chromite and associated silicates are functions of silicate–chromite ratios. There are many gaps, however, in available information.

Systematic investigation of the chromitic rocks of the Critical Zone of the Eastern Bushveld Complex has been under way at the University of Wisconsin for some years. Both chromite and associated silicates in chromite-rich and chromite-poor rocks have been studied. This paper reports on the composition of chromite in the Critical Zone of the central sector of the Eastern Complex, as illustrated in a nearly continuous section of the Zone on Farms Jagdlust, Winterveld, and Umkoanes Stad, and on certain implications for the origin of the chromite deposits.

## Materials studied

The materials studied are from the following sources:

(1) Drillhole U.S. 7, Umkoanes Stad 419 KS, Johannesburg Consolidated Investments, Ltd,
(2) Drillholes 15 and 16, Winterveld 417 KS, Union Carbide Corporation,
(3) Drillholes 8 and 11, Jagdlust 418 KS, Union Carbide Corporation,
(4) Drillhole 17, Jagdlust 418 KS, National Science Foundation,
(5) Mine workings and outcrops: Winterveld, Jagdlust, and Umkoanes Stad.

The locations of the farms named are shown in Figure 1. Together the materials give a composite section of the Critical Zone that is complete except for parts of the lowest few hundred feet, which could be sampled only in discontinuous outcrops. A generalized version of the section is given in Figure 2.

Thin and polished sections have been used as controls on electron microprobe analysis of chromites.

1. Haakdoornhoek 409 KS
2. Jagdlust 418 KS
3. Winterveld 417 KS
4. Zeekoegat 421 KS
5. Umkoanes Stad 419 KS
6. Driekop 253 KT
7. Winterveld 293 KT

Bushveld granite and associated rocks

n    Main norite zone

Critical Zone

Transition Zone and lower rocks

Pretoria Series and associated rocks

Lines of sections on which Figure 2 is based
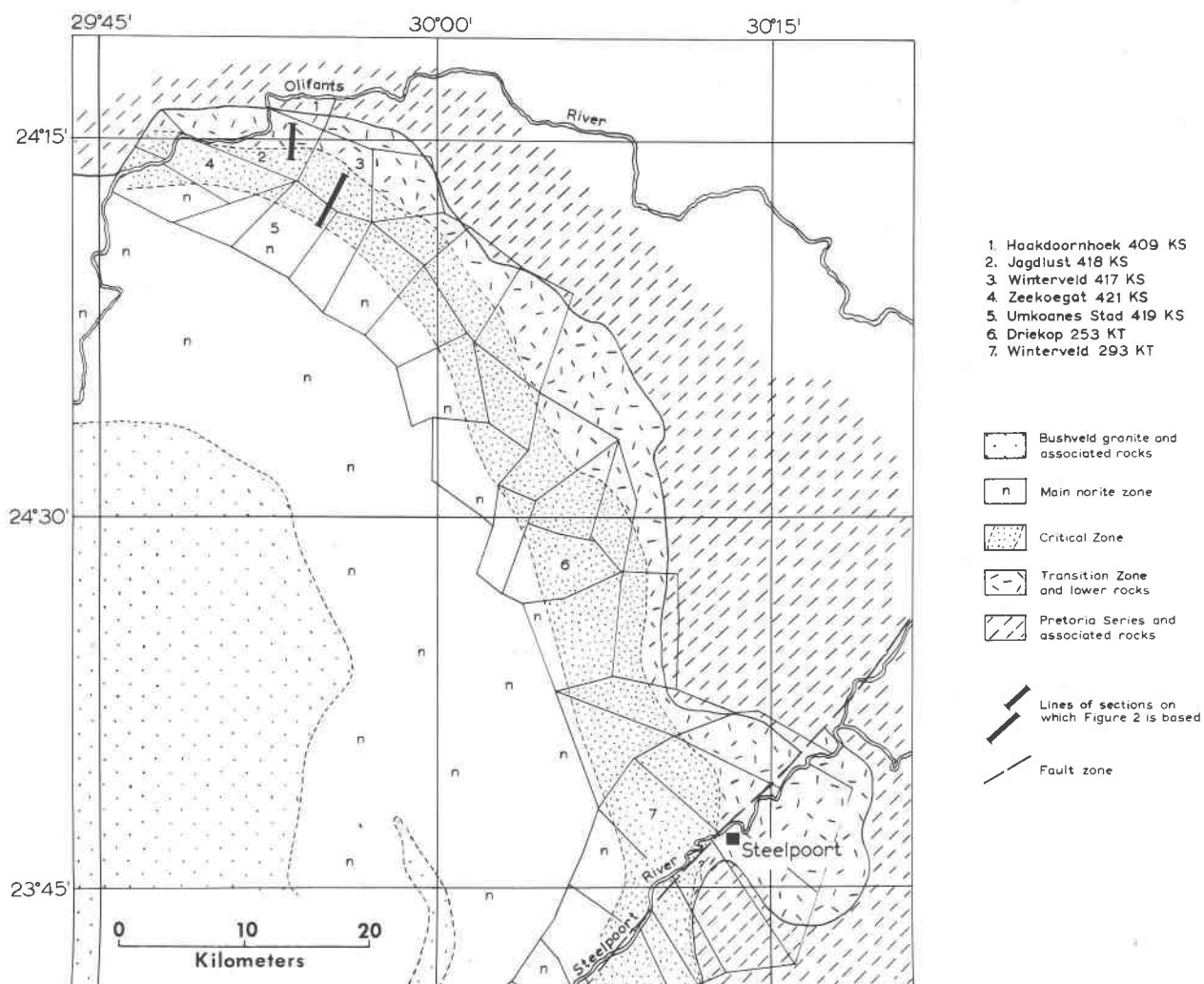
Fault zone

Fig. 1. Index map, showing locations of farms mentioned in the text.

Analyses have been made by methods previously described (Cameron and Glover, 1973). Some analyses were referred to a wet-analyzed chromite, synthetic $TiO_2$, synthetic $Al_2O_3$, an analyzed hematite, vanadium metal, synthetic MgO, and an analyzed rhodonite as standards for Cr, Ti, Al, Fe, V, Mg, and Mn, respectively. More recently, a chromite (Cameron and Emerson, 1959, Table 1, analysis 3) analyzed by C. O. Ingamells has been used as the standard for Cr, Fe, Mg, and Al. This has speeded analysis and, for Al, has eliminated correction problems encountered when synthetic $Al_2O_3$ was used as a standard.

In general, the purpose of analysis has been to determine the average composition of chromite in each sample, by averaging counts made on 6 to 12 randomly-selected chromite grains. For most samples this procedure is satisfactory, because variations

from grain to grain are small. In some samples, however, particularly those in which the modal amount of chromite is a few percent or less, marked variations in composition are found from grain to grain. In such cases, individual grains have been analyzed.

Analysis has generally been restricted to $TiO_2$, $Cr_2O_3$, $Al_2O_3$, FeO, MgO, and $V_2O_3$. $Fe_2O_3$ has been calculated, assuming stoichiometry. Analyses of Bushveld chromites by Waal (1975) show the presence of NiO (0.08 to 0.21 percent), ZnO (0.06 to 0.25 percent), CoO (0.2 percent), and CaO (0.18 to 0.34 percent). Analyses by the writer and other investigators show that MnO is commonly 0.15 to 0.3 percent, rarely 0.4 percent. The writer has generally omitted analysis for these oxides, since the amounts are very small and there appears to be no systematic variation at accuracy levels of microprobe analysis. Many pub-
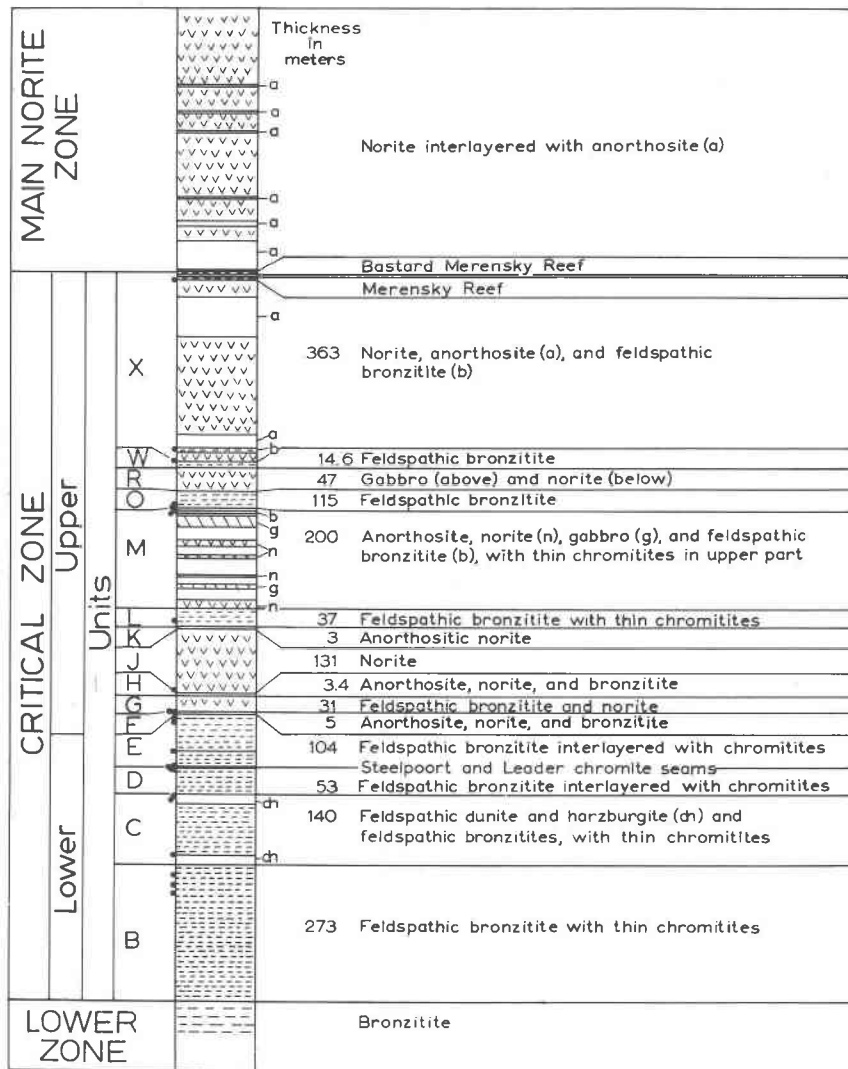
Fig. 2. Generalized stratigraphic sequence in the Critical Zone, on Farms Jagdlust, Winterveld, and Umkoanes Stad. Solid circles along lefthand margin of log indicate positions of chromitites 4 to 26 of Figure 3.

lished analyses of "purified" chromites show small amounts of $SiO_2$, and the analyses reported by Waal (1975) show 0.35 to 1.25 percent in various chromites. The common method of purification is magnetic separation followed by treatment of the chromite concentrate to dissolve unremoved silicates. Results are checked by binocular examination. This method may not always remove all adhering and included silicates. The writer has been unable to detect Si in the chromites analyzed. If Si is present, it must be below 0.1 percent. CaO reported may also be due wholly or in part to impurities.

$TiO_2$ is a special problem. Rutile is present in most chromitic rocks from the Bushveld Complex, partly as inclusions in chromite, partly as marginal adhering grains. Microscope examination of "purified chromite" from rutile-bearing chromitites indicates that adhering rutile is not likely to be totally removed in the purification process, and the rutile inclusions are of course untouched. The relations of rutile to chromite are complex and will be discussed in a separate paper. Meanwhile, it is evident that care must be taken in interpreting $TiO_2$ contents of chromite shown by analyses.

## Occurrence of chromite in the Critical Zone

The occurrence of chromite in the Critical Zone of the central sector of the Eastern Bushveld Complex

has been summarized by various investigators (Kupferberger *et al.,* 1937; Cameron, 1964; Cousins, 1964; Cameron and Desborough, 1969), and only a brief review is given here. Chromite is found in accessory or trace amounts in units that together make up more than half the total thickness of the Critical Zone, but layers containing more than 1 percent chromite are restricted to certain stratigraphic intervals termed "chromitic intervals" (Cameron and Desborough, 1969). For the most part, chromite is a cumulus mineral, but where it is a trace mineral it may be postcumulus. In the true chromitites, chromite is the sole cumulus mineral, except that cumulus rutile occurs in trace amounts in certain chromitites. In other chromitic rocks bronzite, olivine, or plagioclase or, less commonly, both bronzite and plagioclase are also present as cumulus minerals. Postcumulus minerals present in chromitic rocks at various horizons are bronzite, plagioclase, clinopyroxene, biotite, alkali feldspar, and rutile.

True chromitites in the Critical Zone range from less than 1 cm to more than 2 m thick. The thickest chromitite in the section discussed here, the Steelpoort seam (12-33 on Table 1), ranges from 1.2 to 1.3 m in the Jagdlust-Winterveld area. The Marker seam (JM in Table 1) and the Leader seam (11-241-B in Table 1) are respectively 50 cm and 32 cm thick. All other chromitites in the section under discussion are thinner, except possibly a seam poorly exposed in the entrance cut of the Winterveld Mine. It may be 60 cm thick. Waal (1975) has reported that in general the thickness of seams increases upward in the Critical Zone, but no systematic variation in thickness is shown in the section under discussion or in other sections of the Critical Zone of the Eastern Bushveld Complex measured by the writer. Cousins (1964) attempted to define three groups of chromitites, Lower, Middle, and Upper, within each of which the seams (a total of 13 in the three groups) are numbered from lowest to highest. This grouping is only roughly applicable to the section under discussion. In the scheme of Cousins, LG6 is the Steelpoort seam (No. 11 of Fig. 1, this paper), LG7 is the Leader seam (No. 12), and the UG-2 seam is No. 24.

### The composition of chromite—general remarks

The Critical Zone of the Bushveld Complex is considered to have formed by fractional crystallization of mafic magma and gravitative accumulation of successive crops of crystals. If no complications are involved, the resulting pile should show a progressive, systematic change in phase compositions and phase

assemblages. Chromite, being a complex solid-solution series, should be a sensitive indicator of the course of fractionation (Irvine, 1965). The reaction relations of chromite with associated silicates (and rutile), however, complicate the pattern of compositional variation. Variations in composition with modal amounts of coexisting olivine and bronzite are well-established (Van der Walt, 1941; Cameron and Desborough, 1969; Jackson, 1969). Variations in composition of chromite in relation to feldspar also have been noted (Cameron, 1975). All such variations are superimposed on the gross pattern of compositional change upward in the stratigraphic succession.

In view of the influence of modal proportions on the composition of chromite at any given stratigraphic horizon, the writer has analyzed two groups of chromites. One group consists of chromites in true chromitites. The second group consists of chromites in silicate-rich rocks, in which the modal chromite content is 5 percent or less.

Analyses of chromites from 26 true chromitites are given in Table 1. The stratigraphic positions of the chromitites are indicated by the black dots to the left of the log of Figure 2. Variations in cation ratios and Cr/Fe ratios are displayed in Figure 3, in which the samples are arranged in stratigraphic order from bottom to top of the Critical Zone. The highest chromitite is in the Merensky Reef (MR). The Steelpoort Seam (No. 11) serves as the reference horizon. Stratigraphic positions of chromitites 4 to 26 are fixed from drillholes and continuous exposures in the adits on Winterveld and Jagdlust, and from adits in the Merensky Reef. Chromitites 4 to 6 were intersected by a drillhole at the portal of the adit of the Jagdlust Mine. Chromitites 1 to 3 were sampled in a measured section along a line 5 km west of the Jagdlust Mine. The three chromitites occur in the same stratigraphic unit, the B unit, as chromitites 4 to 6, but owing to lack of exposures between drillhole and mine the correlation of the two sets of seams is uncertain.

### Chromite in chromitites

Broadly speaking, the changes in chemistry of chromite in chromitites upward in the Critical Zone are those described in the literature. There is an upward increase in total iron, $Al/R^{3+}$, and $Fe^{3+}/R^{3+}$. The other ratios given in Figure 3 all decrease upward. $TiO_2$ increases irregularly upward, likewise the content of $V_2O_3$. None of the chemical parameters, however, shows a straight-line progression from bottom to top of the stratigraphic sequence.

Table 1. Analyses of chromites from chromitites of the Critical Zone. See text for relations between Nos. 1, 2, and 3 and Nos. 4, 5, and 6.

|  | 26. | 25. | 24. | 23. | 22. | 21. | 20. | 19. | 18. |
|---|---|---|---|---|---|---|---|---|---|
| Sample | 61-46-260 | 15-12B | 15-18 | 15-35-A-2-1 | 15-35-B-2 | 15-36-1 | 15-48 | 15-125-C-2 | 11-15-B |
| $TiO_2$ | 1.29 | 0.62 | 0.89 | 1.01 | 1.24 | 1.19 | 1.14 | 0.93 | 0.97 |
| $FeO^2$ | 23.86 | 22.20 | 19.64 | 22.13 | 22.77 | 21.83 | 23.31 | 21.48 | 23.61 |
| MgO | 7.45 | 8.47 | 10.20 | 8.32 | 8.38 | 9.16 | 7.48 | 9.12 | 7.60 |
| $Cr_2O_3$ | 44.77 | 45.74 | 41.62 | 43.48 | 43.82 | 43.66 | 44.13 | 43.01 | 43.86 |
| $Al_2O_3$ | 13.69 | 16.67 | 16.77 | 15.67 | 15.67 | 15.78 | 14.99 | 17.18 | 16.03 |
| $V_2O_3$ | $0.46^1$ | 0.35 | 0.30 | 0.40 | 0.61 | 0.43 | 0.43 | 0.51 | 0.59 |
| $Fe_2O_3$ | 8.41 | 5.89 | 10.19 | 7.48 | 7.59 | 9.00 | 8.00 | 7.55 | 6.86 |
|  | 99.93 | 99.92 | 99.61 | 98.49 | 100.08 | 101.05 | 99.84 | 99.78 | 99.52 |
| Cations/32O |  |  |  |  |  |  |  |  |  |
| $Ti^{4+}$ | 0.2573 | 0.1205 | 0.1730 | 0.2017 | 0.2444 | 0.2309 | 0.2259 | 0.1799 | 0.1928 |
| $Fe^{2+}$ | 5.3063 | 4.8344 | 4.2448 | 4.9107 | 4.9792 | 4.7094 | 5.1440 | 4.6569 | 5.2072 |
| $Mg^{2+}$ | 2.9510 | 3.2861 | 3.9282 | 3.2910 | 3.2652 | 3.5215 | 3.0818 | 3.5230 | 2.9856 |
| $Cr^{3+}$ | 9.4118 | 9.4168 | 8.5025 | 9.1177 | 9.0583 | 8.9036 | 9.2067 | 8.8131 | 9.1438 |
| $Al^{3+}$ | 4.2917 | 5.1155 | 5.1079 | 4.9001 | 4.8320 | 4.7980 | 4.6617 | 5.2487 | 4.9839 |
| $V^{3+}$ | $0.0980^2$ | 0.0731 | 0.0622 | 0.0849 | 0.1271 | 0.0889 | 0.0916 | 0.1052 | 0.1250 |
| $Fe^{3+}$ | 1.6839 | 1.1537 | 1.9815 | 1.4938 | 1.4937 | 1.7477 | 1.5883 | 1.4732 | 1.3617 |
|  | 24.0000 | 24.0001 | 24.0001 | 23.9999 | 23.9999 | 24.0000 | 24.0000 | 24.0000 | 24.0000 |
| Cr/Fe (wt. %) | 1.22 | 1.43 | 1.27 | 1.33 | 1.30 | 1.28 | 1.27 | 1.34 | 1.32 |
| Cation ratios |  |  |  |  |  |  |  |  |  |
| $Mg/Mg+Fe^{2+}$ | 0.357 | 0.405 | 0.481 | 0.401 | 0.396 | 0.428 | 0.375 | 0.431 | 0.364 |
| $Cr/Cr+Al+Fe^{3+}$ | 0.612 | 0.600 | 0.545 | 0.588 | 0.589 | 0.576 | 0.596 | 0.567 | 0.590 |
| $Al/Cr+Al+Fe^{3+}$ | 0.279 | 0.326 | 0.328 | 0.316 | 0.314 | 0.310 | 0.302 | 0.338 | 0.322 |
| $Fe^{3+}/Cr+Al+Fe^{3+}$ | 0.109 | 0.074 | 0.129 | 0.096 | 0.097 | 0.113 | 0.103 | 0.095 | 0.088 |

[1]Value for MnO.    [2]Value for $Mn^{2+}$.   V not determined.

|  | 17. | 16. | 15. | 14. | 13. | 12. | 11. | 10. | 9. |
|---|---|---|---|---|---|---|---|---|---|
| Sample | 8-146 | 11-165-1 | 15-148 | 15-1983 | J.M. | 11-241* | 12-33 | J-40 | W-53-23 |
| $TiO_2$ | 0.67 | 0.72 | 0.75 | 0.84 | 0.63 | 0.58 | 0.61 | 0.55 | 0.52 |
| $FeO^2$ | 19.54 | 20.84 | 20.70 | 19.83 | 20.18 | 19.03 | 19.22 | 18.96 | 17.99 |
| MgO | 10.23 | 9.60 | 9.57 | 10.02 | 9.53 | 10.07 | 10.20 | 10.21 | 10.82 |
| $Cr_2O_3$ | 42.16 | 42.18 | 43.04 | 43.36 | 46.45 | 47.31 | 47.42 | 47.70 | 49.43 |
| $Al_2O_3$ | 18.00 | 13.30 | 17.95 | 16.70 | 14.26 | 14.49 | 14.83 | 14.48 | 14.67 |
| $V_2O_3$ | 0.47 | 0.37 | 0.33 | 0.33 | 0.38 | 0.23 | 0.27 | 0.27 | 0.22 |
| $Fe_2O_3$ | 8.27 | 8.11 | 7.25 | 8.32 | 8.54 | 7.44 | 7.35 | 7.31 | 5.61 |
|  | 99.34 | 100.12 | 99.15 | 99.39 | 99.97 | 99.15 | 99.89 | 99.48 | 99.26 |
| Cations/32O |  |  |  |  |  |  |  |  |  |
| $Ti^{4+}$ | 0.1301 | 0.1379 | 0.1449 | 0.1639 | 0.1230 | 0.0621 | 0.1230 | 0.1087 | 0.1015 |
| $Fe^{2+}$ | 4.2070 | 4.4693 | 4.4660 | 4.2965 | 4.4110 | 4.1430 | 4.1728 | 4.1383 | 3.9108 |
| $Mg^{2+}$ | 3.9231 | 3.6686 | 3.6789 | 3.8674 | 3.7120 | 3.9088 | 3.9423 | 3.9704 | 4.1919 |
| $Cr^{3+}$ | 8.5804 | 8.5501 | 8.7761 | 8.8826 | 9.5994 | 9.7340 | 9.7324 | 9.8386 | 10.1580 |
| $Al^{3+}$ | 5.4602 | 5.5322 | 5.4586 | 5.0989 | 4.3943 | 4.5102 | 4.5365 | 4.4518 | 4.4949 |
| $V^{3+}$ | 0.0974 | 0.0769 | 0.0676 | 0.0684 | 0.0798 | 0.0500 | 0.0568 | 0.0563 | 0.0469 |
| $Fe^{3+}$ | 1.6018 | 1.5651 | 1.4079 | 1.6224 | 1.6806 | 1.4580 | 1.4362 | 1.4360 | 1.0964 |
|  | 24.0000 | 24.0001 | 24.0000 | 24.0001 | 24.0001 | 23.8653 | 24.0000 | 24.0001 | 24.0004 |
| Cr/Fe (wt. %) | 1.38 | 1.32 | 1.39 | 1.40 | 1.49 | 1.62 | 1.62 | 1.64 | 1.89 |
| Cation ratios |  |  |  |  |  |  |  |  |  |
| $Mg/Mg+Fe^{2+}$ | 0.483 | 0.451 | 0.452 | 0.473 | 0.463 | 0.485 | 0.485 | 0.490 | 0.517 |
| $Cr/Cr+Al+Fe^{3+}$ | 0.548 | 0.546 | 0.561 | 0.569 | 0.612 | 0.620 | 0.620 | 0.626 | 0.645 |
| $Al/Cr+Al+Fe^{3+}$ | 0.349 | 0.354 | 0.349 | 0.327 | 0.280 | 0.287 | 0.289 | 0.283 | 0.285 |
| $Fe^{3+}/Cr+Al+Fe^{3+}$ | 0.102 | 0.100 | 0.090 | 0.104 | 0.107 | 0.093 | 0.091 | 0.091 | 0.070 |

*Wet chemical analysis, C. O. Ingamells.   Also contains 0.44% MnO.

Table 1. Continued

| | 8. | 7. | 6. | 5. | 4. | 3. | 2. | 1. |
|---|---|---|---|---|---|---|---|---|
| Sample | 61-46-291A | 61-46-297 | 17-151-10 | 17-204-8 | 17-222 | 75-24 | 75-23 | 75-22 |
| $TiO_2$ | 0.76 | 0.46 | 0.52 | 0.58 | 0.76 | 0.48 | 0.51 | 0.55 |
| $FeO^2$ | 18.64 | 17.84 | 18.55 | 18.90 | 19.07 | 17.90 | 18.90 | 17.96 |
| $MgO$ | 10.48 | 10.78 | 10.23 | 10.08 | 9.98 | 10.56 | 10.09 | 10.55 |
| $Cr_2O_3$ | 50.13 | 49.95 | 49.88 | 48.89 | 49.23 | 50.66 | 49.91 | 49.92 |
| $Al_2O_3$ | 13.75 | 13.72 | 13.16 | 13.33 | 13.20 | 12.54 | 13.43 | 13.23 |
| $V_2O_3$ | 0.44 | 0.23 | 0.26 | 0.26 | 0.45 | 0.21 | 0.29 | 0.25 |
| $Fe_2O_3$ | 5.23 | 6.30 | 6.41 | 7.08 | 6.01 | 6.61 | 6.13 | 6.11 |
| | 99.43 | 99.28 | 99.01 | 99.12 | 98.70 | 98.96 | 99.26 | 98.57 |
| **Cations/32O** | | | | | | | | |
| $Ti^{4+}$ | 0.1491 | 0.0910 | 0.1027 | 0.1154 | 0.1504 | 0.0950 | 0.1016 | 0.1081 |
| $Fe^{2+}$ | 4.0718 | 3.8961 | 4.0864 | 4.1613 | 4.2187 | 3.9466 | 4.1530 | 3.9609 |
| $Mg^{2+}$ | 4.0773 | 4.1949 | 4.0162 | 3.9541 | 3.9317 | 4.1484 | 4.0132 | 4.1472 |
| $Cr^{3+}$ | 10.3491 | 10.3104 | 10.3846 | 10.1749 | 10.2922 | 10.5587 | 10.3656 | 10.4067 |
| $Al^{3+}$ | 4.2330 | 4.2226 | 4.0856 | 4.1376 | 4.1158 | 3.8969 | 4.1592 | 4.1132 |
| $V^{3+}$ | 0.0911 | 0.0473 | 0.0543 | 0.0540 | 0.0946 | 0.0434 | 0.0602 | 0.0523 |
| $Fe^{3+}$ | 1.0286 | 1.2379 | 1.2701 | 1.4026 | 1.1966 | 1.3109 | 1.2116 | 1.2116 |
| | 24.0000 | 24.0002 | 23.9999 | 23.9999 | 24.0000 | 23.9999 | 23.9999 | 24.0000 |
| $Cr/Fe$ (wt. %) | 1.89 | 1.87 | 1.81 | 1.70 | 1.77 | 1.87 | 1.80 | 1.87 |
| **Cation ratios** | | | | | | | | |
| $Mg/Mg+Fe^{2+}$ | 0.500 | 0.518 | 0.496 | 0.487 | 0.482 | 0.512 | 0.487 | 0.511 |
| $Cr/Cr+Al+Fe^{3+}$ | 0.663 | 0.654 | 0.660 | 0.647 | 0.660 | 0.670 | 0.659 | 0.662 |
| $Al/Cr+Al+Fe^{3+}$ | 0.271 | 0.268 | 0.260 | 0.263 | 0.264 | 0.247 | 0.264 | 0.261 |
| $Fe^{3+}/Cr+Al+Fe^{3+}$ | 0.066 | 0.078 | 0.081 | 0.089 | 0.077 | 0.083 | 0.077 | 0.077 |

The most nearly systematic variation is shown by the chromitites of the Lower Critical Zone. It should be noted that there are two groups of chromitites in this part of the Critical Zone. One group, represented by samples 7, 8, and 9, consists of chromitites in olivine-rich rocks. The second group, represented by all the other samples from 1 to 15, consists of chromitites enclosed in bronzitites. The second group shows a fairly regular progression in chromite composition upward. Total iron, $Al/R^{3+}$, and $Fe^{3+}/R^{3+}$ increase upward, whereas $Cr/Fe$, $Mg/(Mg + Fe^{2+})$, and $Cr/R^{3+}$ decline. The three chromitites enclosed in olivine-rich rocks show higher MgO, Cr/Fe, and $Cr_2O_3$, and lower total Fe than chromitites in bronzitites above and below.

In the Lower Critical Zone, plagioclase is post-cumulus (Cameron, 1969). Modal plagioclase content in bronzitites increases upward to 17 to 18 percent near the top of the zone, indicating that as the zone accumulated the composition of the magma was gradually approaching the bronzite–plagioclase boundary on the liquidus. The top of the Lower Critical Zone is an erosional disconformity (Cameron, 1971), above which cumulus plagioclase appears for the first time. Strong movement of magma just prior to the beginning of accumulation of the F

unit is indicated, but trends of bronzite composition do not indicate a heave of new magma into the chamber (Cameron, 1971). Analyses and cation ratios for chromitites 15 and 16 (Table 1 and Fig. 3) show no break in compositional trends across the disconformity.

The top part of the E unit is an alternation of parallel, regular, concordant layers of chromitite, chromitic bronzitite, and bronzitite. Chromitites 13 and 14 from this sequence differ somewhat in composition, but there is no evidence of a break in the sequence, either in the field or in analyses of bronzites (Cameron, 1971, Fig. 14) from various horizons in the sequence.

The Upper and Lower Critical Zones of the central sector of the Eastern Bushveld Complex are lithologically different. The Lower Critical Zone is essentially a pile of feldspathic bronzitites interrupted by two horizons (upper and lower members of the C unit) of peridotitic rocks, and chromitic intervals in this pile are rather closely spaced. The Upper Critical Zone is a very diverse assemblage of norites, anorthosites, minor gabbros, and bronzitites, in which chromitic intervals are fewer. The chromitites of the Upper Critical Zone occur in three types of associations with silicate rocks. The chromitites represented by Nos.
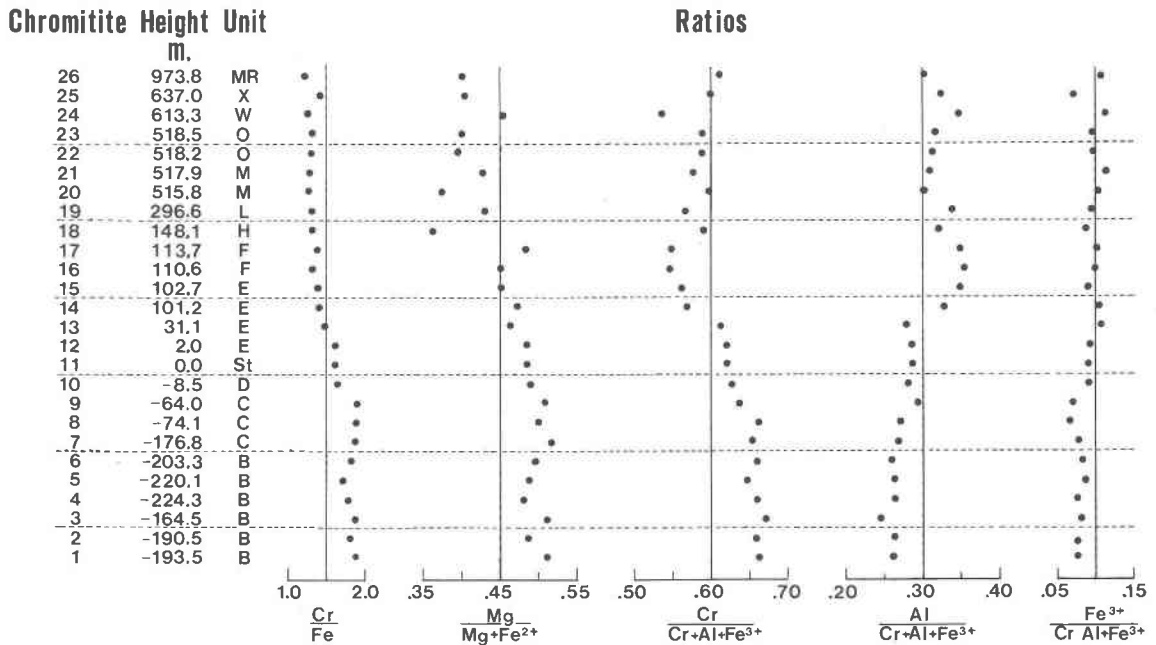
Fig. 3. Cr/Fe and selected cation ratios for 26 chromitites. Stratigraphic positions are given in meters above or below the Steelpoort chromitite. Sample numbers are those of Table 1. Chromitites 4 to 26 are in stratigraphic order. See text for relations of chromitites 1 to 3 to chromitites 4 to 6.

18, 19, 22, 23, 24, and 26 (Table 1 and Fig. 3) are enclosed in feldspathic bronzitites. Nos. 20 and 21 are from a series of thin chromitites interlayered with anorthosites at the top of the M unit. Nos. 16, 17, and 25 are from chromitites each of which is underlain by anorthosite and overlain by bronzitite. Whether taken as a whole or in groups according to type of associated silicate rock, the chromitites show no systematic variation upward with stratigraphic position. For example, the $Mg/R^{2+}$ ratio of chromite in No. 24 is almost identical with that of No. 17, whereas chromites in intervening chromitites have much lower ratios. It should be noted that in chromitites the variations from grain to grain are small, and replicate analyses agree within limits of error of microprobe analysis.

From the chart it seems clear that if the compositions of successive chromitites reflect the differentiation of the magma, the course of differentiation of the Upper Critical Zone was by no means simple. This is also suggested by the repetition of rock types and rock sequences in the Upper Critical Zone.

In Figure 4, $Cr^{3+}/R^{3+}$ is plotted against $Mg/R^{2+}$ for chromites in chromitites of the Lower and Upper Critical Zones. Chromite in chromitites of the Lower Critical Zone in bronzitites in general shows a decrease in $Cr^{3+}/R^{3+}$ with decrease in $Mg/R^{2+}$. For

chromite in chromitites enclosed in dunites there is no clear trend. The reverse trend, however, is shown by chromitites of the Upper Critical Zone, whether or not they are enclosed in pyroxenite or are enclosed in or underlain by anorthosite. Trends for $Al/R^{3+}$ plotted against $Mg/R^{2+}$ (Fig. 5) are antithetic to trends in $Cr/R^{3+}$.

### Chromite in chromite-poor rocks

Chromites from silicate-rich rocks at 38 stratigraphic horizons have been analyzed. Cr/Fe and cation ratios are plotted in Figure 6 in stratigraphic order. Compared to chromites in chromitites, chromites in silicate-rich rocks in general have lower $Mg/R^{2+}$, $Al/R^{3+}$, and Cr/Fe, and higher $Cr/R^{3+}$ and $Fe^{3+}/R^{3+}$. This corresponds to relative enrichment in $FeCr_2O_4$. Trends in composition upward in the stratigraphic column are obscured by the scattering of values. In part this certainly reflects variations in composition from grain to grain in many single samples. The range in sample no. 5 (Nos. 5a and 5b of Table 2) is given as an extreme but informative illustration. In this sample, 5 grains embedded in bronzite show essentially the same range as 5 grains embedded in plagioclase, hence subsolidus equilibration does not appear to have been the cause. It seems more likely that variations are due to point-to-point varia-

tions in the composition of interstitial liquid, which was separated into innumerable isolated subsystems in the last stages of crystallization. In any event, it is clear that only analyses of large numbers of grains in each individual sample would indicate average compositions of chromites.

So far as trends in ratios are discernible, those in Figure 6 seem to parallel those in Figure 3, except that the $Al/R^{3+}$ ratios in Figure 6 show little change, and there appears to be a reversal in $Fe^{3+}/R^{3+}$ in the part of the Lower Critical Zone made up of the B, C, and D units.

### Chromites in chromitite–silicate rock series

Three types of chromitite–silicate rock series, based on variations in modal proportions, are present in the Critical Zone—chromitite–bronzitite, chromitite–dunite, and chromitite–anorthosite. Chromitite–dunite series are present only in the C and D units, Lower Critical Zone. Chromitite–bronzitite

Fig. 5. $Al/(Cr + Al + Fe^{3+})$ for the chromitites of Table 1 plotted against $Mg/(Mg + Fe^{2+})$. Symbols as in Figure 4.
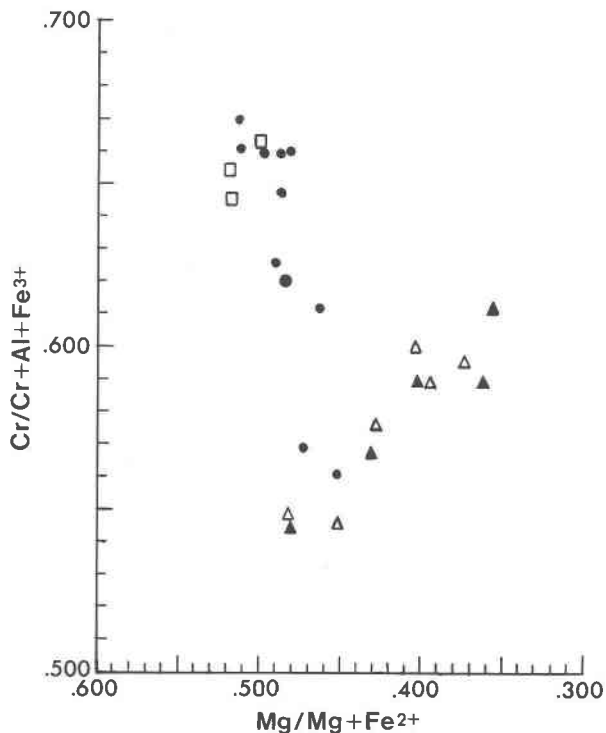
Fig. 4. $Cr/(Cr + Al + Fe^{3+})$ for the chromitites of Table 1, plotted against $Mg/(Mg + Fe^{2+})$. Chromitites in the Lower Critical Zone are represented by solid circles (chromitites enclosed in bronzitites) and rectangles (chromitites enclosed in olivine-rich rocks). The large circle represents both Steelport and Leader chromitites. Chromitites in the Upper Critical Zone are represented by triangles, open (chromitites enclosed in anorthosite or in anorthosite and bronzitite) or solid (chromitites enclosed in bronzitite).
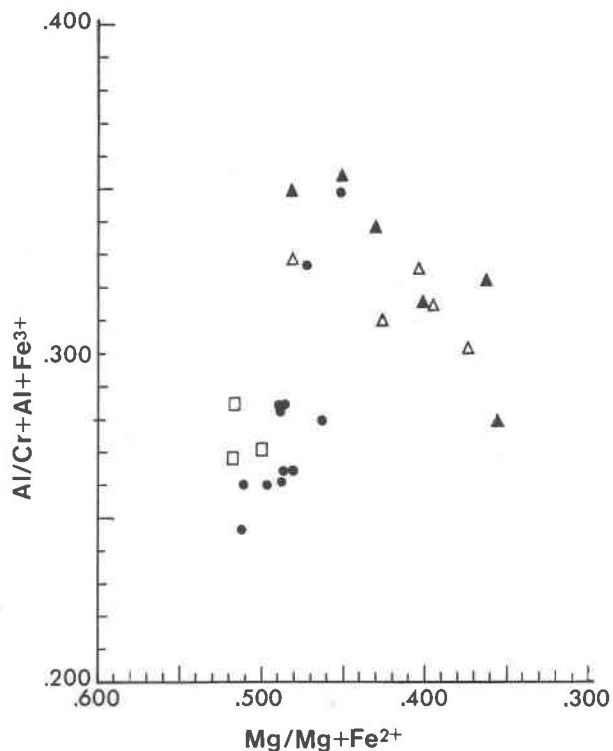
series are found at intervals from bottom to top of the Lower Critical Zone, and in certain bronzitites of the W, O, L, and lower J units. Chromitite–anorthosite series are found only in the M, H, and F units.

Patterns of variation in the composition of chromite in chromitite–bronzitite series have been described by Cameron and Desborough (1969) and Cameron (1970). As chromite–bronzite ratios increase, there is an increase in $Mg/R^{2+}$, $Cr/Fe$, and $Al/R^{3+}$ ratios, and a decrease in other ratios. The variation in $Mg/R^{2+}$ was first noted by Van der Walt (1941) in chromitic rocks of the Western Bushveld Complex.

Patterns of variation in chromitite–dunite series in the Western Bushveld Complex have been studied by G. von Gruenewaldt (personal communication, 1975), who finds that the $Al/R^{3+}$ ratio decreases with increasing chromite content, the reverse of the change in chromitite–bronzitite series. The chemical relationships involved will be discussed by Dr. von Gruenewaldt in a forthcoming paper. Similar series in the C unit subsequently investigated by the author show the same variation. Thus chromite in chromitite No. 7 (Table 1) has an $Al/R^{3+}$ ratio of 0.268, whereas chro-
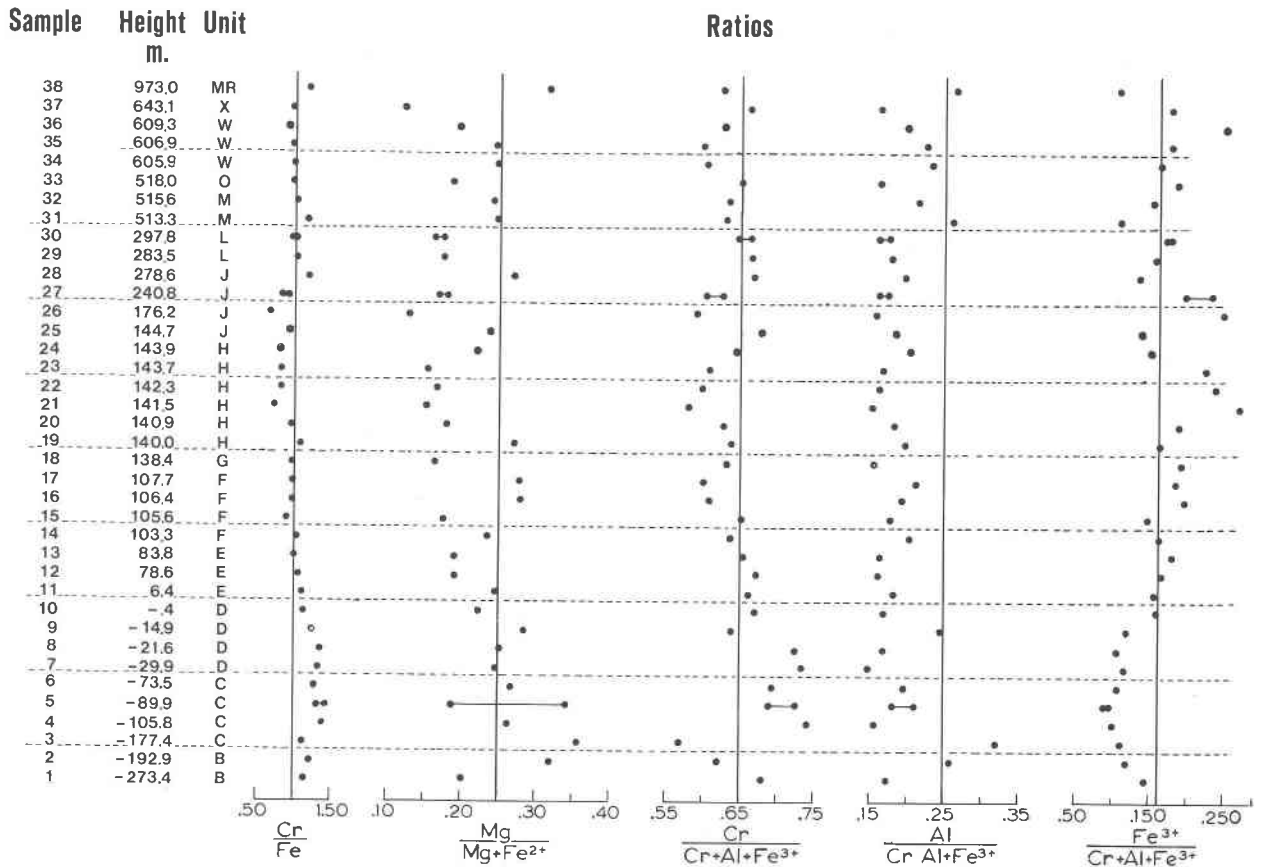
Fig. 6. Cr/Fe and selected cation ratios for chromites in silicate-rich rocks of Table 2. Stratigraphic positions are referred to the Steelpoort chromitite. Sample numbers are those of Table 2.

mite from the associated dunite of sample 3 (Table 2) has a ratio of 0.320.

The pattern of chemical variation in chromitite–anorthosite series has been described by the writer (Cameron, 1975), and is indicated by a comparison of the cation ratios of No. 21, Table 1 (chromite in chromitite), and No. 32, Table 2 (accessory chromite in the underlying anorthosite). $Mg/R^{2+}$ and $Al/R^{3+}$ are higher in chromite from the chromitite. In these respects the pattern is similar to that in chromitite–bronzitite series, but in chromitite–anorthosite series Cr/Fe may either increase with modal percent chromite, decrease, or remain the same.

### Discussion

The significance of the compositional data presented here depends on whether the compositions of the chromites were fixed during crystallization of the magma or during the succeeding subsolidus stage. This question was examined in a previous paper

(Cameron, 1975). In any given chromitite, chromite is in places poikilitic in plagioclase, in other places poikilitic in bronzite. If subsolidus equilibration has taken place, chromite in bronzite should have a lower Mg/Fe ratio than chromite surrounded by plagioclase (Irvine, 1967). Analyses show that this is not the case, hence the composition of chromite was fixed not later than the end of the postcumulus state of crystallization, in a system in which chromite, plagioclase, bronzite, and liquid were in equilibrium. Variations in composition of chromite upward in the stratigraphic sequence should therefore reflect the fractionation of the magma.

The most distinct fractionation apparently took place during the formation of the Lower Critical Zone and the lowest unit, the F unit, of the Upper Critical Zone. Crystallization of bronzite, olivine, and chromite depleted the magma in Mg, Fe, and Cr. Mg was depleted relative to Fe. The $Mg/R^{2+}$, Cr/Fe, and $Cr^{3+}/R^{3+}$ ratios in chromite therefore de-

Table 2. Analyses of chromites from silicate-rich rocks of the Critical Zone

| | 38. | 37. | 36. | 35. | 34. | 33. | 32. | 31. |
|---|---|---|---|---|---|---|---|---|
| Sample | 61-46-260 | 15-9A | 15-204 | 15-213 | 15-200 | 15-34-A-2 | 15-37-B | 15-80 |
| $TiO_2$ | 0.70 | 0.65 | 1.28 | 1.18 | 1.22 | 1.54 | 1.54 | 1.49 |
| $FeO$ | 24.67 | 29.82 | 28.14 | 27.16 | 27.04 | 28.58 | 27.16 | 26.58 |
| $MgO$ | 6.39 | 2.32 | 3.83 | 4.94 | 5.02 | 3.66 | 4.87 | 5.59 |
| $Cr_2O_3$ | 45.81 | 45.57 | 42.92 | 42.63 | 42.92 | 44.23 | 44.04 | 44.72 |
| $Al_2O_3$ | 13.09 | 7.42 | 7.96 | 10.68 | 11.03 | 7.36 | 9.94 | 12.37 |
| $V_2O_3$ | 0.41 | 0.53 | 0.51 | 0.39 | 0.43 | 0.57 | 0.47 | 0.64 |
| $Fe_2O_3$ | 8.27 | 12.83 | 14.48 | 13.27 | 12.27 | 13.25 | 11.14 | 8.23 |
| Totals | 99.34 | 99.14 | 99.12 | 100.26 | 99.93 | 99.19 | 99.16 | 99.62 |
| Cations/32 O | | | | | | | | |
| $Ti^{4+}$ | 0.1431 | 0.1392 | 0.2731 | 0.2437 | 0.2511 | 0.3291 | 0.3227 | 0.3040 |
| $Fe^{2+}$ | 5.5711 | 7.1487 | 6.6583 | 6.2255 | 6.2012 | 6.7803 | 6.3074 | 6.0405 |
| $Mg^{2+}$ | 2.5721 | .9906 | 1.6148 | 2.0182 | 2.0498 | 1.5489 | 2.0153 | 2.2635 |
| $Cr^{3+}$ | 9.7769 | 10.3263 | 9.6010 | 9.2378 | 9.3051 | 9.9205 | 9.6693 | 9.6070 |
| $Al^{3+}$ | 4.1664 | 2.5058 | 2.6551 | 3.4510 | 3.5656 | 2.4629 | 3.2539 | 3.9626 |
| $V^{3+}$ | 0.0896 | 0.1216 | 0.1146 | 0.0861 | 0.0943 | 0.1305 | 0.1041 | 0.1387 |
| $Fe^{3+}$ | 1.6809 | 2.7668 | 3.0831 | 2.7377 | 2.5329 | 2.8279 | 2.3275 | 1.6837 |
| Totals | 24.0001 | 23.9999 | 24.0000 | 24.0000 | 24.0000 | 24.0001 | 24.0002 | 24.0000 |
| Cr/Fe (wt. %) | 1.26 | 0.99 | 0.92 | 0.96 | 0.99 | 0.96 | 1.04 | 1.16 |
| Cation ratios | | | | | | | | |
| $Mg/Mg+Fe^{2+}$ | 0.316 | 0.248 | 0.195 | 0.245 | 0.248 | 0.186 | 0.242 | 0.273 |
| $Cr/Cr+Al+Fe^{3+}$ | 0.626 | 0.604 | 0.626 | 0.599 | 0.604 | 0.656 | 0.634 | 0.630 |
| $Al/Cr+Al+Fe^{3+}$ | 0.267 | 0.232 | 0.173 | 0.224 | 0.232 | 0.162 | 0.213 | 0.260 |
| $Fe^{3+}/Cr+Al+Fe^{3+}$ | 0.108 | 0.164 | 0.201 | 0.178 | 0.164 | 0.186 | 0.153 | 0.110 |

| | 30. | 29. | 28. | 27. | 26. | 25. | 24. | 23. |
|---|---|---|---|---|---|---|---|---|
| Sample | 15-1300 | 15-1349 | 15-1367-2 | 15-1600[1] | 15-1725 | 8-4-C | 8-18 | 8-27 |
| $TiO_2$ | 1.11 | 1.21 | 1.10 | 1.11 | 0.92 | 1.36 | 1.09 | 1.58 |
| $FeO$ | 28.81 | 28.76 | 25.91 | 28.66 | 29.61 | 27.02 | 26.82 | 29.79 |
| $MgO$ | 3.44 | 3.42 | 5.40 | 3.34 | 2.47 | 4.77 | 4.91 | 3.20 |
| $Cr_2O_3$ | 44.71 | 45.62 | 47.00 | 42.27 | 39.99 | 46.99 | 45.39 | 41.13 |
| $Al_2O_3$ | 8.06 | 8.19 | 9.28 | 7.48 | 7.17 | 8.54 | 9.63 | 7.59 |
| $V_2O_3$ | 0.16 | 0.59 | 0.65 | 0.77 | 0.90 | 0.71 | 0.67 | 0.74 |
| $Fe_2O_3$ | 12.90 | 11.28 | 9.99 | 15.55 | 17.70 | 10.02 | 11.22 | 15.96 |
| Totals | 99.71 | 99.07 | 99.33 | 99.18 | 98.66 | 99.01 | 99.73 | 99.99 |
| Cations/32 O | | | | | | | | |
| $Ti^{4+}$ | 0.2349 | 0.2567 | 0.2287 | 0.2382 | 0.1998 | 0.2843 | 0.2275 | 0.3368 |
| $Fe^{2+}$ | 6.7916 | 6.8135 | 5.9997 | 6.8199 | 7.1389 | 6.3020 | 6.2037 | 7.0611 |
| $Mg^{2+}$ | 1.4432 | 1.4432 | 2.2290 | 1.4183 | 1.0609 | 1.9824 | 2.0238 | 1.2756 |
| $Cr^{3+}$ | 9.9616 | 10.2153 | 10.2873 | 9.5104 | 9.1149 | 10.3610 | 9.9241 | 9.2173 |
| $Al^{3+}$ | 2.6772 | 2.7333 | 3.0295 | 2.5075 | 2.4359 | 2.8085 | 3.1394 | 2.5352 |
| $V^{3+}$ | 0.1560 | 0.1330 | 0.1434 | 0.1752 | 0.2087 | 0.1584 | 0.1470 | 0.1683 |
| $Fe^{3+}$ | 2.7354 | 2.4051 | 2.0823 | 3.3306 | 3.8409 | 2.1034 | 2.3345 | 3.4056 |
| Totals | 23.9999 | 24.0001 | 23.9999 | 24.0001 | 24.0000 | 24.0000 | 24.0000 | 23.9999 |
| Cr/Fe (wt. %) | 0.97 | 1.03 | 1.19 | 0.87 | 0.77 | 0.95 | 0.82 | 0.82 |
| Cation ratios | | | | | | | | |
| $Mg/Mg+Fe^{2+}$ | 0.175 | 0.175 | 0.271 | 0.172 | 0.129 | 0.239 | 0.246 | 0.153 |
| $Cr/Cr+Al+Fe^{3+}$ | 0.648 | 0.665 | 0.668 | 0.620 | 0.592 | 0.678 | 0.645 | 0.608 |
| $Al/Cr+Al+Fe^{3+}$ | 0.174 | 0.178 | 0.197 | 0.163 | 0.158 | 0.184 | 0.204 | 0.167 |
| $Fe^{3+}/Cr+Al+Fe^{3+}$ | 0.178 | 0.157 | 0.135 | 0.217 | 0.250 | 0.138 | 0.152 | 0.225 |

[1] Average of analyses of six crystals

Table 2. Continued

|  | 22. | 21. | 20. | 19. | 18. | 17. | 16. | 15. |
|---|---|---|---|---|---|---|---|---|
| Sample | 8-52 | 8-66 | 11-64-B | 8-91 | 15-1870 | 8-141 | 11-1-40 | 11-154 |
| $TiO_2$ | 1.31 | 1.30 | 1.04 | 1.10 | 0.84 | 0.95 | 0.92 | 0.57 |
| FeO | 28.91 | 29.35 | 27.37 | 26.00 | 28.83 | 26.24 | 25.49 | 28.37 |
| MgO | 3.26 | 2.94 | 4.25 | 5.43 | 3.16 | 5.61 | 5.53 | 3.37 |
| $Cr_2O_3$ | 40.59 | 38.98 | 43.57 | 45.14 | 45.20 | 43.68 | 43.21 | 45.36 |
| $Al_2O_3$ | 7.37 | 6.85 | 8.47 | 9.35 | 7.06 | 10.32 | 9.15 | 8.26 |
| $V_2O_3$ | 0.74 | 0.96 | 0.65 | 0.66 | 0.87 | 0.54 | 0.42 | 0.93 |
| $Fe_2O_3$ | 16.97 | 18.96 | 13.87 | 12.14 | 13.80 | 14.14 | 14.72 | 12.55 |
| Totals | 99.13 | 99.34 | 99.21 | 99.82 | 99.76 | 101.48 | 99.44 | 99.41 |
| Cations/32 O |  |  |  |  |  |  |  |  |
| $Ti^{4+}$ | 0.2804 | 0.2808 | 0.2197 | 0.2278 | 0.1783 | 0.1923 | 0.1913 | 0.1216 |
| $Fe^{2+}$ | 6.8937 | 7.0275 | 6.4314 | 5.9949 | 6.8419 | 5.9321 | 5.9070 | 6.7013 |
| $Mg^{2+}$ | 1.3867 | 1.2533 | 1.7883 | 2.2329 | 1.3364 | 2.2602 | 2.2844 | 1.4204 |
| $Cr^{3+}$ | 9.1507 | 8.8211 | 9.6771 | 9.8395 | 10.1388 | 9.3350 | 9.4658 | 10.1283 |
| $Al^{3+}$ | 2.4785 | 2.3125 | 2.8059 | 3.0396 | 2.3606 | 3.2885 | 2.9884 | 2.7497 |
| $V^{3+}$ | 0.1689 | 0.2192 | 0.1457 | 0.1456 | 0.1969 | 0.1162 | 0.0930 | 0.2113 |
| $Fe^{3+}$ | 3.6411 | 4.0856 | 2.9320 | 2.5198 | 2.9472 | 2.8758 | 3.0701 | 2.6675 |
| Totals | 23.9999 | 24.0000 | 24.0001 | 24.0001 | 24.0001 | 24.0001 | 24.0000 | 24.0001 |
| Cr/Fe (wt. %) | 0.81 | 0.74 | 0.96 | 1.08 | 0.96 | 0.96 | 0.98 | 0.90 |
| Cation ratios |  |  |  |  |  |  |  |  |
| $Mg/Mg+Fe^{2+}$ | 0.167 | 0.151 | 0.179 | 0.271 | 0.163 | 0.276 | 0.279 | 0.175 |
| $Cr/Cr+Al+Fe^{3+}$ | 0.599 | 0.580 | 0.628 | 0.639 | 0.656 | 0.602 | 0.610 | 0.652 |
| $Al/Cr+Al+Fe^{3+}$ | 0.162 | 0.152 | 0.182 | 0.197 | 0.153 | 0.212 | 0.192 | 0.177 |
| $Fe^{3+}/Cr+Al+Fe^{3+}$ | 0.238 | 0.269 | 0.190 | 0.164 | 0.151 | 0.185 | 0.198 | 0.172 |

|  | 14. | 13. | 12. | 11. | 10. | 9. | 8. | 7. |
|---|---|---|---|---|---|---|---|---|
| Sample | 11-161 | 15-2047 | 15-2067 | J-15-2316 | 12-42-1 | 69-23 | 65-27 | 65-29 |
| $TiO_2$ | 1.02 | 0.77 | 0.72 | 0.83 | 0.21 | 0.71 | 0.74 | 0.91 |
| FeO | 27.05 | 27.99 | 27.71 | 26.54 | 26.49 | 25.71 | 26.04 | 26.22 |
| MgO | 4.67 | 3.69 | 3.65 | 4.90 | 4.30 | 5.63 | 4.93 | 4.78 |
| $Cr_2O_3$ | 44.84 | 45.52 | 46.45 | 46.95 | 47.68 | 46.83 | 51.11 | 51.15 |
| $Al_2O_3$ | 9.54 | 7.62 | 7.45 | 8.68 | 8.01 | 11.92 | 8.01 | 6.97 |
| $V_2O_3$ | 0.48 | 0.71 | 0.64 | 0.42 | 0.44 | 0.38 | 0.35 | 0.45 |
| $Fe_2O_3$ | 11.97 | 13.23 | 12.03 | 11.68 | 11.95 | 8.34 | 7.84 | 8.74 |
| Totals | 99.57 | 99.53 | 98.65 | 100.00 | 98.88 | 99.52 | 99.02 | 99.94 |
| Cations/32 O |  |  |  |  |  |  |  |  |
| $Ti^{4+}$ | 0.2129 | 0.1634 | 0.1553 | 0.1736 | 0.0451 | 0.1455 | 0.1550 | 0.1924 |
| $Fe^{2+}$ | 6.2809 | 6.6107 | 6.6042 | 6.1515 | 6.2407 | 5.8591 | 6.0982 | 6.1837 |
| $Mg^{2+}$ | 1.9320 | 1.5527 | 1.5510 | 2.0221 | 1.8043 | 2.2864 | 2.0568 | 2.0087 |
| $Cr^{3+}$ | 9.8429 | 10.1630 | 10.4634 | 10.2865 | 10.6179 | 10.0882 | 11.3153 | 11.3996 |
| $Al^{3+}$ | 3.1221 | 2.5381 | 2.5007 | 2.8365 | 2.6597 | 3.8286 | 2.6435 | 2.3162 |
| $V^{3+}$ | 0.1071 | 0.1571 | 0.1463 | 0.0927 | 0.1000 | 0.0830 | 0.0779 | 0.1014 |
| $Fe^{3+}$ | 2.5021 | 2.8125 | 2.5790 | 2.4371 | 2.5322 | 1.7092 | 1.6532 | 1.7980 |
| Totals | 24.0000 | 23.9975 | 23.9999 | 24.0000 | 23.9999 | 24.0000 | 23.9999 | 24.0000 |
| Cr/Fe (wt. %) | 1.04 | 1.00 | 1.06 | 1.12 | 1.13 | 1.22 | 1.36 | 1.33 |
| Cation ratios |  |  |  |  |  |  |  |  |
| $Mg/Mg+Fe^{2+}$ | 0.235 | 0.190 | 0.190 | 0.247 | 0.224 | 0.281 | 0.252 | 0.245 |
| $Cr/Cr+Al+Fe^{3+}$ | 0.636 | 0.655 | 0.673 | 0.661 | 0.671 | 0.646 | 0.725 | 0.735 |
| $Al/Cr+Al+Fe^{3+}$ | 0.202 | 0.164 | 0.161 | 0.182 | 0.168 | 0.245 | 0.169 | 0.149 |
| $Fe^{3+}/Cr+Al+Fe^{3+}$ | 0.162 | 0.181 | 0.166 | 0.157 | 0.160 | 0.109 | 0.106 | 0.116 |

Table 2. Continued

|  | 6. | 5a.* | 5b. | 4. | 3. | 2. | 1. |
|---|---|---|---|---|---|---|---|
| Sample | 61-46-290 | 61-46-293 | 61-46-293 | 61-46-295 | 16-302-2 | 17-110 | 17-416 |
| $TiO_2$ | 0.72 | 0.32 | 0.89 | 1.07 | 0.77 | 0.53 | 0.31 |
| FeO | 25.77 | 28.07 | 23.72 | 26.04 | 23.71 | 24.33 | 27.33 |
| MgO | 5.23 | 3.58 | 7.04 | 5.20 | 7.45 | 6.43 | 3.88 |
| $Cr_2O_3$ | 49.52 | 51.90 | 50.46 | 52.15 | 42.78 | 45.72 | 48.32 |
| $Al_2O_3$ | 9.35 | 8.73 | 10.40 | 7.34 | 16.10 | 12.71 | 8.27 |
| $V_2O_3$ | 0.40 | 0.33 | 0.32 | 0.38 | 0.21 | 0.24 | 0.37 |
| $Fe_2O_3$ | 8.05 | 6.75 | 7.40 | 7.54 | 8.74 | 9.23 | 10.77 |
| Totals | 99.04 | 99.68 | 100.23 | 99.72 | 99.76 | 99.19 | 99.25 |
| Cations/32 O |  |  |  |  |  |  |  |
| $Ti^{4+}$ | 0.1496 | 0.0672 | 0.1806 | 0.2239 | 0.1519 | 0.1078 | 0.0653 |
| $Fe^{2+}$ | 5.9848 | 6.5745 | 5.3504 | 6.0650 | 5.2262 | 5.5121 | 6.4355 |
| $Mg^{2+}$ | 2.1647 | 1.4927 | 2.8302 | 2.1588 | 2.9256 | 2.5957 | 1.6298 |
| $Cr^{3+}$ | 10.8704 | 11.4893 | 10.7603 | 11.4803 | 8.9154 | 9.7912 | 10.7567 |
| $Al^{3+}$ | 3.0588 | 2.8804 | 3.3062 | 2.4082 | 5.0036 | 4.0587 | 2.7457 |
| $V^{3+}$ | 0.0892 | 0.0738 | 0.0694 | 0.0844 | 0.0449 | 0.0522 | 0.0845 |
| $Fe^{3+}$ | 1.6824 | 1.4223 | 1.5028 | 1.5793 | 1.7334 | 1.8823 | 2.2824 |
| Totals | 23.9999 | 24.0002 | 23.9999 | 23.9999 | 24.0000 | 24.0000 | 23.9999 |
| Cr/Fe (wt. %) | 1.28 | 1.34 | 1.46 | 1.40 | 1.19 | 1.23 | 1.15 |
| Cation ratios |  |  |  |  |  |  |  |
| $Mg/Mg+Fe^{2+}$ | 0.266 | 0.185 | 0.346 | 0.263 | 0.359 | 0.320 | 0.202 |
| $Cr/Cr+Al+Fe^{3+}$ | 0.696 | 0.727 | 0.691 | 0.742 | 0.570 | 0.622 | 0.681 |
| $Al/Cr+Al+Fe^{3+}$ | 0.196 | 0.182 | 0.212 | 0.156 | 0.320 | 0.258 | 0.174 |
| $Fe^{3+}/Cr+Al+Fe^{3+}$ | 0.108 | 0.090 | 0.097 | 0.102 | 0.111 | 0.120 | 0.145 |

* 5a and 5b are analyses of two different crystals.

creased, especially in the E unit of the Lower Critical Zone, whereas the $Al^{3+}/R^{3+}$ and $Fe^{3+}/R^{3+}$ ratios rose.

After the completion of the F unit (No. 17, Table 1), the pattern of fractionation changed. Cr/Fe remained essentially constant. $Mg/R^{2+}$ shows a wide fluctuation from chromitite to chromitite, but on the whole there is little change. The same is true for the $Fe^{3+}/R^{3+}$ ratio. The removal of large amounts of $Al_2O_3$ in plagioclase during the accumulation of the Upper Critical Zone is apparently reflected in reversal of the trend of the $Cr^{3+}/R^{3+}$ and $Al^{3+}/R^{3+}$ ratios.

Deviations of individual values from general trends in the Upper Critical Zone do not correlate with either kinds or proportions of silicates in the chromitites or in the immediately enclosing silicate rocks. The rocks of the Upper Critical Zone are predominantly noritic, but the recurrence of pyroxenites in the sequence indicates periodic change in the position of the system relative to the bronzite–plagioclase boundary on the liquidus. Chromite was only intermittently a stable phase. It is absent in the thick J unit, and in most of the M and X units (Fig. 2),

except as a trace mineral that may be of postcumulus origin.

The chromitite of No. 24 (UG-2 of Cousins' scheme) is markedly aberrant in $Mg/R^{2+}$, $Cr^{3+}/R^{3+}$, and $Fe^{3+}/R^{3+}$ ratios. The data are from one of four separate analyses, two for chromite poikilitically enclosed in plagioclase, two of chromite poikilitically enclosed in bronzite, that are in very close agreement. No explanation is apparent. A heave of undifferentiated magma into the chamber is suggested by the relatively high $Mg/R^{2+}$ ratio, but the shifts in the other ratios are opposite to what would be expected if a heave had taken place.

It is apparent from Figures 5 and 6 that none of the ratios can be used to fix the exact position of a chromitite in the stratigraphic sequence. However, $Cr^{3+}/R^{3+}$ and $Al^{3+}/R^{3+}$ relative to $Mg/R^{2+}$ serve to distinguish chromitites of the Upper Critical Zone from those of the Lower Critical Zone.

For the chromites in chromite-poor rocks, two features require explanation. One is the strong enrichment in iron, titanium, and to a less extent, vanadium, relative to chromites in chromitites at the same horizons. The second is the marked scattering

of values, to such a degree that trends of certain ratios (Fig. 6) are obscured.

The contrasts in composition could conceivably stem from the cumulus stage, and there is no proof that they do not. They could also reflect, however, the reaction of settled chromite, initially of the same composition as chromite forming adjacent chromitite, with interstitial liquid during the postcumulus stage. Such a liquid would be enriched in Fe, Ti, and V relative to cumulus chromite. Since the ratio of liquid to chromite would be high, substantial change in chromite composition could occur, whereas it would not occur in chromitites, in which chromite/liquid ratios would be high. In the last stages, if interstitial liquid became restricted to very small volumes isolated from one another, reaction of liquid with some chromite crystals might continue much longer than with others, and the chromite/liquid ratios might vary from volume to volume. The range of composition of crystals in some of the chromite-poor rocks could thus be explained.

As Irvine (1965) has pointed out, chromitic spinels should be sensitive indicators of conditions of magma crystallization. In experimental systems in which the changes in cation ratios in spinels can be correlated specifically with changes in bulk composition, temperature, or oxygen fugacity, there is ample evidence that phase compositions are markedly affected by changes in one or more of those variables. In the system $MgO-FeO-Fe_2O_3-SiO_2$, the Mg/Fe ratios of both spinel and coexisting olivine or orthopyroxene increase with increase in oxygen fugacity of the liquid (Muan and Osborn, 1956; Ulmer, 1969). In addition, increase in oxygen fugacity (Kennedy, 1955; Osborn, 1959; Hamilton et al., 1964; Yoder and Tilley, 1962) promotes the crystallization of spinel at the expense of silicates. Cameron and Desborough (1969) and Ulmer (1969) therefore suggested that the chromitic intervals in the Critical Zone were initiated by increase in oxygen fugacity and terminated by decrease in oxygen fugacity. Both the formation of chromitites and the variations in Mg/Fe ratio in coexisting chromite and olivine or bronzite could thus be explained. Cameron and Desborough pointed out, however, that the higher $Al_2O_3$ content of chromite in the chromitites is anomalous, since in the system $FeO-Fe_2O_3-Al_2O_3-SiO_2$ (Muan, 1957) increase in $fO_2$ causes a decrease in the $Al_2O_3$ content of spinel.

The difficulty lies in attempting to extrapolate from the relatively simple experimental systems to the more complex natural systems, particularly those in which the spinel phase contains Cr, $Fe^{2+}$, $Fe^{3+}$, Mg, Al, and Ti in significant amounts, and in which temperature, oxygen fugacity, and bulk composition have yet to be defined.

In this connection, the work of Hill and Roeder (1974) on the crystallization of spinel from a basaltic liquid produced by melting a Hawaiian olivine–tholeiite is of special interest. In one set of runs, spinel was crystallized from the basaltic liquid at a temperature of $1200° \pm 6°$ C, over a range of oxygen fugacity from about $10^{-0.4}$ to $10^{-9}$. In the second set of runs, spinels were crystallized at a constant oxygen fugacity of $10^{-7}$ over the temperature range from about $1202°$ to $1147°$ C. Compositions of the resulting spinels were determined by microprobe analysis. At $1200°$ C, increase in oxygen fugacity did promote the crystallization of spinel, but the $Al_2O_3$ content of spinel decreased and so did the Cr/Fe and $Mg/R^{2+}$ ratios. For $Mg/R^{2+}$, this statement holds only for the range of $fO_2$ from $10^{-7}$ to $10^{-9}$, but this is the range considered most likely for mafic magmas at $1200°$ C (Fudali, 1965). The change in $Al_2O_3$ content is thus consistent with relations in the system $FeO-Fe_2O_3-Al_2O_3-SiO_2$ (Muan, 1957), but the change in $Mg/R^{2+}$ is opposite to that which occurs in the system $MgO-FeO-Fe_2O_3-SiO_2$ (Muan and Osborn, 1956).

If the findings of Hill and Roeder can be extrapolated to the Bushveld magma system, doubt is cast on the role of oxygen fugacity in the crystallization of chromite. For any given pair of layers consisting of a chromitite and a chromite-poor silicate rock, it seems reasonable to assume that the two crystallized at essentially the same temperature. If formation of the chromitite was caused by increase in $fO_2$, $Al_2O_3$ content and the ratios Cr/Fe and $Mg/R^{2+}$ should all be lower in chromite from the chromitite, the reverse of what is found in the Critical Zone.

The control of chromitite formation by oxygen fugacity has been questioned on other grounds. The hypothesis was proposed at a time when the mafic belts of the Bushveld were considered to be parts of a single complex, and the remarkable similarity of the eastern and western belts did not seem inconsistent with the hypothesis. It is now established that the eastern and western belts were intruded from separate centers. Dr. C. F. Vermaak (personal communication, 1975) points out that there is small likelihood that variations in oxygen fugacity would occur at closely similar stages in the eastern and western complexes. The same problem must be considered in evaluating the contamination hypothesis proposed by Irvine (1975). There is also the problem posed by the

large number of chromitites present in the Critical Zone. Osborn (1969) has pointed out that it is difficult to visualize a mechanism by which numerous variations in oxygen fugacity could be produced.

An equally serious problem is the persistence of certain of the chromitites. The Marker, Leader, and Steelpoort chromitites, and a chromitite about 8.5 m. below the Steelpoort chromitite (Nos. 13, 12, 11, and 10, respectively, in Fig. 3) are known to extend from Jagdlust nearly 60 km southward to the Steelpoort River. Some of the other chromitites, less well exposed, may be equally persistent. Development of such persistent units would seem to require, at specific stages in the evolution of the Critical Zone, changes in the magma system that were established rapidly and uniformly over long distances.

Irvine (1975) showed experimentally that contamination of the parental magma with granitic melt derived from roof rocks could cause precipitation of chromite. He proposed this as the mechanism by which chromitites have formed in the Muskox and other layered intrusions. More recently (Irvine, 1977), he has proposed an alternative hypothesis that chromitites form when chromite-saturated picritic tholeiite liquid is blended with the earlier liquid of the same type that has differentiated to relatively siliceous compositions. Applied to the chromitites of the Busveld Complex, both modes of origin require very rapid and very uniform mixing of new liquid with magma already present in the chamber, not once but a number of times. To the writer it seems very unlikely that such mixing could take place over distances of tens of kilometers, hence some other mechanism of chromitite formation must be sought.

There is one change in a magma system that could be produced rapidly and uniformly in a huge magma chamber, namely, change in total pressure (liquestatic pressure) due to tectonism affecting the magma chamber during crystallization. There is evidence of such tectonism during formation of the Eastern Bushveld Complex (Cameron, 1977). During much of the crystallization of the Critical Zone, the system was close to the boundary of the chromite field on the liquidus. Osborn (1977) has shown that in the system $MgO-FeO-Fe_2O_3-SiO_2-CaAl_2Si_2O_8$, the experimental system most closely approaching basaltic magma, change in total pressure shifts phase boundaries on the liquidus. In a system on or close to a phase boundary, change in pressure due to tectonism might suffice to induce a change in the phase or phases precipitating.

If neither oxygen fugacity nor subsolidus equilibra-

tion is the cause of covariation in compositions of chromite and silicates, we require some other explanation. The only one at hand was offered long ago by Van der Walt (1941), who first recognized covariation of the ratio $Mg/Fe^{2+}$ in the bronzitite–chromitite series of the Western Bushveld Complex. He wrote (p. 105):

"That the chromite in the silicate rocks is richer in FeO and poorer in MgO than the (chromite in the) chromitite bands, is due to the fact that the chromite of the silicate bands has crystallized simultaneously with a relative abundance of pyroxenes. The latter minerals used up a relatively large amount of MgO, so that the ratio of FeO to MgO in the residual magma increased and the chromite, when then formed from it, had to reflect a content of FeO higher than obtained in the bands of chromite."

Similar reasoning can be used to explain the fact that in chromitite–anorthosite series in the $Al_2O_3$ content of chromite increases with modal percent chromite. The variations in $Al_2O_3$ content of chromite in chromitite–bronzitite and chromitite–dunite series, however, remain unexplained. It seems evident that additional experimental work is needed.

## Acknowledgments

## References

Cameron, E. N. (1964) Chromite deposits of the eastern part of the Bushveld Complex. In S. H. Haughton, Ed., *The Geology of Some Ore Deposits of Southern Africa,* Vol. 2, Geol. Soc. S. Africa, 131–168.
——— (1969) Postcumulus changes in the eastern Bushveld Complex. *Am. Mineral., 54,* 754–779.
——— (1970) Compositions of certain coexisting phases in the eastern part of the Bushveld Complex. *Geol. Soc. South Africa Spec. Pap., 1,* 46–58.

——— (1971) Problems of the Eastern Bushveld Complex. *Fortschr. Mineral., 48,* 86–108.

——— (1975) Postcumulus and subsolidus equilibration of chromite and coexisting silicates in the Eastern Bushveld Complex. *Geochim. Cosmochim. Acta, 39,* 1021–1033.

——— (1977) The Lower Zone of the Eastern Bushveld Complex in the Olifants River Trough. *J. Petrol.,* in press.

——— and M. E. Emerson (1959) The origin of certain chromite deposits in the eastern part of the Bushveld Complex. *Econ. Geol., 54,* 1151–1213.

——— and G. A. Desborough (1969) Occurrence and characteristics of chromite deposits—eastern Bushveld Complex. *Econ. Geol., Mon. 4,* 23–40.

——— and E. D. Glover (1973) Unusual titanian–chromian spinels from the Eastern Bushveld Complex. *Am. Mineral., 58,* 172–188.

Cousins, C. A. (1964) Additional notes on the chromite deposits of the eastern part of the Bushveld Complex. In S. H. Haughton, Ed., *The Geology of Some Ore Deposits of Southern Africa,* Vol. Geol. Soc. S. Africa, 2, 169–182.

Fudali, R. F. (1965) Oxygen fugacities of basaltic and andesitic magmas. *Geochim. Cosmochim. Acta, 29,* 1063–1075.

Hamilton, D. L., C. W. Burnham and E. F. Osborn (1964) The solubility of water and effects of oxygen fugacity and water content on crystallization in mafic magmas. *J. Petrol., 5,* 21–38.

Hill, R. and P. Roeder (1974) The crystallization of spinel from basaltic magma as a function of oxygen fugacity. *J. Geol., 82,* 709–729.

Irvine, T. N. (1965) Chromian spinel as a petrogenetic indicator, Part I. Theory. *Can. J. Earth Sci., 2,* 648–672.

——— (1967) Chromian spinel as a petrogenetic indicator, Part 2. Petrologic applications. *Can. J. Earth Sci., 4,* 71–103.

——— (1975) Crystallization sequences in the Muskox intrusion and other layered intrusions, II. Origin of chromitite layers and similar deposits of other magmatic ores. *Geochim. Cosmochim. Acta, 39,* 991–1020.

——— (1977) Origin of chromitite layers in the Muskox intrusion and other stratiform intrusions: a new interpretation. *Geology, 5,* 273–277.

Jackson, E. D. (1969) Chemical variation in coexisting chromite and olivine in chromitite zones of the Stillwater Complex. *Econ. Geol., Mon. 4,* 41–71.

Kennedy, G. C. (1955) Some aspects of the role of water in igneous melts. *Geol. Soc. Am. Spec. Pap., 62,* 489–503.

Kupferberger, W., B. V. Lombaard, B. Wasserstein and C. M. Schwellnus (1937) The chromite deposits of the Bushveld Igneous Complex, Transvaal. *Bull. Geol. Surv. S. Africa, 10,* 48 p.

Muan, A. (1957) Phase equilibrium relationships at liquidus temperatures in the system $FeO-Fe_2O_3-Al_2O_3-SiO_2$. *J. Am. Ceram. Soc., 40,* 420–431.

——— and E. F. Osborn (1956) Phase equilibria at liquidus temperatures in the system $MgO-FeO-Fe_2O_3-SiO_2$. *J. Am. Ceram. Soc., 39,* 121–140.

Osborn, E. F. (1959) Role of oxygen pressure in the crystallization and differentiation of basaltic magma. *Am. J. Sci., 257,* 609–647.

——— (1969) Discussion of Ulmer, G. C. (1969), Experimental investigations of chromite spinels. *Econ. Geol., Mon. 4,* 131.

——— (1977) Origin of calc-alkali magma series of Santorini Volcano type in the light of recent experimental phase-equilibrium studies. *Proceedings, International Congress on Thermal Waters, Geothermal Energy, and Vulcanism of the Mediterranean Area,* Athens, Greece, October 11, 1976, in press.

Ulmer, G. C. (1969) Experimental investigations of chromite spinels. *Econ. Geol., Mon. 4,* 114–181.

Van der Walt, C. F. J. (1941) Chrome ores of the western Bushveld Complex. *Trans. Geol. Soc. S. Africa, XLIV,* 79–112.

Waal, S. A. de (1975) The mineralogy, chemistry, and certain aspects of reactivity of chromitite from the Bushveld igneous complex. *National Institute for Metallurgy, Johannesburg, Rep. 1709,* 80 p.

Yoder, H. S. and C. E. Tilley (1962) Origin of basalt magmas: an experimental study of natural and synthetic rock systems. *J. Petrol., 3,* 342–532.